Physical Chemistry 2026, 14(1): 1-9
DOI: 10.5923/j.pc.20261401.01

Oxalic Acid Functionalized Diatomite for Enhanced Lead (II) ions Adsorption from Wastewater

Winny Chebeni Masai, Francis Maingi*, Maximilla Makhanu

Department of Science Technology and Engineering, Kibabii University, Kenya

Abstract Increased global demand for batteries and paints has resulted in higher levels of heavy-metal contamination in waterways, harming aquatic life and human health. Lead is of particular concern due to its non-biodegradable nature and persistence at trace levels. Various technologies have been developed for heavy metal removal from wastewater, with adsorption being the most effective and resource-efficient. Information in literature shows that diatomite has the ability to adsorb heavy metal ions from aqueous media but suffers from a low adsorption capacity and specific surface area. This study therefore focused on enhancing the adsorption capacity of low-cost diatomite by functionalizing it with carboxyl groups via oxalic acid. Characterization techniques, including XRF, FT-IR, XRD, and Raman spectroscopy, confirmed the successful functionalization. Batch adsorption experiments demonstrated that functionalized diatomite effectively removed over 80% of Pb (II) ions, with an adsorption capacity of 8.00 mg/g. These findings suggest that functionalized diatomite is a promising potential adsorbent for remediation of heavy metal ions from wastewater.

Keywords Adsorption, Diatomite, Functionalized, Lead, Wastewater

1. Introduction

Water pollution is a serious environmental concern in Kenya, which has been exacerbated by industrialization, population increase, agriculture, and lack of proper waste management practices [1]. Heavy metals and other contaminants pose significant danger to the environment, water supplies, and human health, making water treatment and water purification systems an important and valuable tool. Water contamination by heavy metals like lead, copper, cadmium, and nickel is a serious environmental issue due to their persistence and non-biodegradability [2]. Heavy metal contamination poses serious environmental and health risks to both human and aquatic life. Various methods for wastewater treatment have been developed, with adsorption being the most effective for removing these metals. Diatomite is a naturally occurring, inexpensive siliceous material with high surface area and porous, making it a promising adsorbent. The hydroxyl groups on the surface of diatomite help improve its ability to stick heavy metal ions to its surface [3]. However, it suffers from low adsorption capacity and specific surface area. This study functionalized raw diatomite from Kariandusi, Kenya, with oxalic acid with the aim of improving its adsorption capacity and specific surface area. Functionalization of diatomite with oxalic acid further increases its adsorption capacity by introducing carboxylate groups that form stable complexes with divalent heavy metal cations, thereby improving its efficacy in water purification applications.

* Corresponding author:
mukoramaingi@gmail.com (Francis Maingi)
Received: Jun. 22, 2026; Accepted: Jul. 13, 2026; Published: Jul. 15, 2026
Published online at http://journal.sapub.org/pc

2. Materials and Methods

2.1. Chemicals and Reagents

The oxalic acid was used in the functionalization of the natural diatomite. Lead (II) nitrate and distilled water were used for the preparation of synthetic wastewater, and NaOH or HCl was used for the pH adjustment. All reagents were of analytical grade.

2.2. Functionalization of Diatomite

The wet functionalization method was used to functionalize raw diatomite in this study. Diatomite was pre-treated with 0.5 M oxalic acid solution. For effective functionalization, the mixture was shaken for 24 hours at room temperature using an orbital shaker. The slurry was then filtered using Whatman No. 41 filter paper and then washed several times with distilled water to rid of excess oxalic acid that may not be chemically bound with diatomite. Functionalized diatomite was later dried at 105℃ for 12 hours in an oven. The sample was then grinded and sieved and stored in a desiccator [4].

2.3. Characterization of the Adsorbents

The characterization of adsorbents is a crucial initial step

in adsorption studies because it connects material properties with adsorption performance. This process explores retention mechanisms, particularly the interaction between adsorbent surfaces and target pollutants, by assessing key physical and chemical properties. The XRF, XRD, FT-IR, and Raman spectroscopic techniques were used to characterize natural and functionalized diatomite in this study.

2.4. Preparation of Pb (II) Ions Sorbates for Adsorption Studies

Stock solutions for adsorption studies were prepared using lead (II) nitrate, which was of analytical grade. A lead (II) ions solution was prepared by dissolving an accurate quantity of 1.559 g of lead (II) nitrate in 500 mL of distilled water and diluting to 1000 mL. The solution was coded as 1000 ppm of Pb (II) ions. The stock solutions were serially diluted to yield working solutions.

2.5. Optimization of Sorption Parameters

2.5.1. Effect of pH on Adsorption of Pb (II) Ions

Study experiments were carried out by varying pH from 2 to 6 using 0.1 M NaOH and 0.1 M HCl to study Pb (II) ions, keeping other conditions constant. 50 mL solutions of 100 mg/L Pb (II) ions were placed in 100 mL bottles containing 0.10 g of functionalized diatomite composite. The bottles were then shaken at 120 rpm for one hour at room temperature, with experiments conducted in triplicate. After shaking, the mixture was filtered, and residual metal ions were analyzed using AAS [5].

2.5.2. Effect of Adsorbent Dose on Adsorption of Pb (II) Ions

The study was conducted to investigate the adsorption of Pb (II) ions by varying the adsorbent dose from 0.02 to 0.20 g while keeping other conditions constant. Solutions containing 100 mg/L of each ion in monocomponent systems were placed in stoppered plastic bottles with different masses of functionalized diatomite composite. The samples were shaken at 120 rpm for one hour in triplicate [5].

2.5.3. Effect of Contact Time on Adsorption of Pb^{2+} Ions

50 mL solutions containing 100 mg/L of Pb (II) ions were mixed with 0.10 g of functionalized diatomite composite in plastic bottles and shaken at 120 rpm. The test was performed in triplicate, and samples were taken at specific intervals ranging from 10 to 120 minutes and then filtered to evaluate residual metal ions using AAS.

2.5.4. Effect of Temperature on Adsorption of Pb (II) Ions

Batch experiments were carried out while varying the temperature between 25 and 45 ℃ while keeping other variables constant. 50 mL solutions of 100 mg/L Pb (II) ions were placed in 100 mL stoppered plastic bottles, to which 0.10 g of a functionalized diatomite composite was added. Bottles were shaken at 120 rpm for one hour in a temperature -controlled shaker. The experiment was conducted in triplicate, and the mean values were used for calculations. After shaking, the supernatant was filtered, and the residual metal ions were analyzed using AAS.

2.5.5. Effect of initial Concentration on Adsorption of Pb(II) Ions

The effect of initial metal ion concentration was conducted by varying the Pb (II) ion concentrations from 25 to 200 mg/L while keeping other conditions constant. Solutions were placed in 100 mL bottles, to which 0.10 g of functionalized diatomite composite was added. The bottles were shaken at 120 rpm and 25 ℃ for one hour. Triplicates were performed, and mean values were calculated. After shaking, supernatants were filtered, and residual metal ions were analyzed using AAS.

2.6. Adsorption isotherms

Adsorption data of the adsorption of Pb (II) ions was fitted in both Freundlich and Langmuir isotherm models to assess the adsorption capacity of functionalized diatomite. The residual metal ion concentrations were measured using AAS, with the equilibrium adsorption (q_e) amount calculated by Equation 1 [6].

$$q_e = \left[\frac{C_0 - C_e}{W}\right]\mathrm{V} \quad (1)$$

Where Co and Ce (mg/L) represent the initial and equilibrium concentrations of the corresponding metal ions, respectively. W (g) is the mass of the dry adsorbent employed, and V is the volume of the solution used (L). Equation 2 shows the linearized Freundlich isotherm used in this study.

$$lnq_e = lnK_F + \frac{1}{n} lnC_e \quad (2)$$

Where: K_F= Freundlich isotherm constant associated with adsorption capacity, q_e = adsorption at equilibrium, 1/n= Heterogeneity index associated with adsorption intensity and C_e = concentration of the adsorbate in solution at equilibrium. Equation 3 shows the linearized Langmuir adsorption isotherm.

$$\frac{C_e}{q_e} = \frac{C_e}{q_m} + \frac{1}{K_L q_m} \quad (3)$$

Where, C_e is the concentration of metal ions at equilibrium (mg/dm^3); q_e is the amount of Pb (II) ions adsorbed (mg/g); q_m is the adsorption capacities (mg/g); K_L is the isotherm constant (dm^3 /mg) [7].

3. Results and Discussions

3.1. XRF Analysis of the Adsorbents

The X-ray fluorescence spectrometer (model S1 Titan) was used to determine the chemical composition of natural and functionalized diatomite. Table 1 shows the chemical composition of both natural and functionalized diatomite.

The study reveals that silica (SiO_2) and (Al_2O_3) are the primary component of both natural and functionalized

diatomite, with contents of 92.583% and 88.611%, 2.8609% and 3.688%, respectively, indicating that both natural and functionalized diatomite are aluminosilicate and functionalization did not alter the structure. Other components include. Fe (2.254%, 3.369%), and Ca (1.090%, 2.284%), which enhance adsorption capacity through ion exchange.

Table 1. Mean percentage chemical composition of natural and functionalized diatomite

Elements Oxides	Natural diatomite Mean% ± SD	Oxalic- acid Functionalized diatomite Mean% ± SD
Al_2O_3	2.860 ±0.237	3.688 ±0.226
SiO_2	92.583 ±0.762	88. 611 ±0.617
P	0.082 ±0.024	0.064 ±0.022
S	0.021 ±0.019	0.105 ±0.019
Cl	0.094 ±0.027	0.112 ±0.026
K_2O	0.779 ±0.021	0.892 ±0.018
Ca	1.090 ±0.069	2.284 ±0.080
Ti	0.103 ±0.015	0.082 ±0.012
V	0.001 ±0.006	0.002 ±0.005
Mn	0.038 ±0.005	0.065 ±0.005
Fe	2.254 ±0.024	3.369 ±0.027

SD- Standard deviation

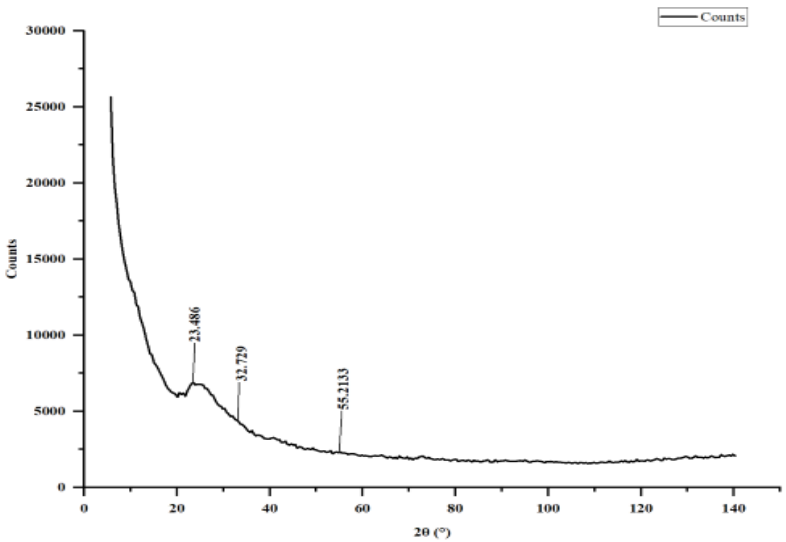

Figure 1. XRD diffraction patterns of natural diatomite

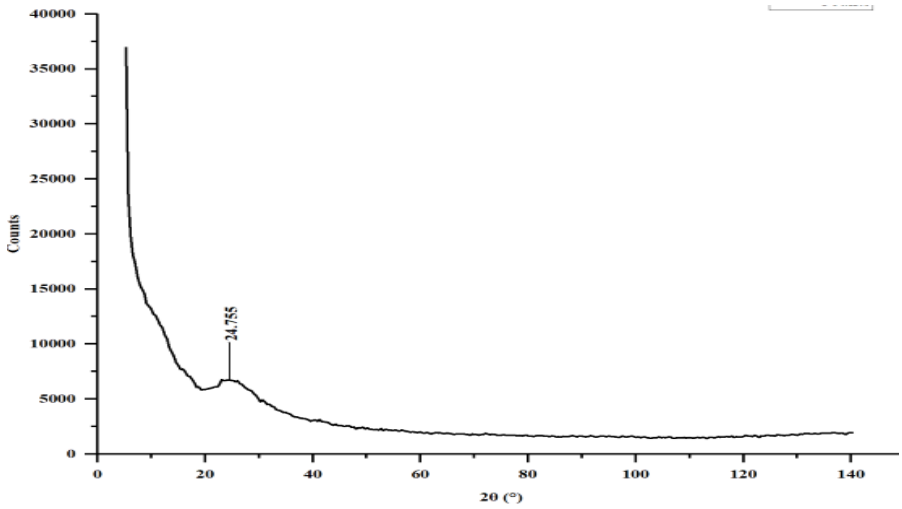

Figure 2. XRD diffraction pattern of functionalized diatomite

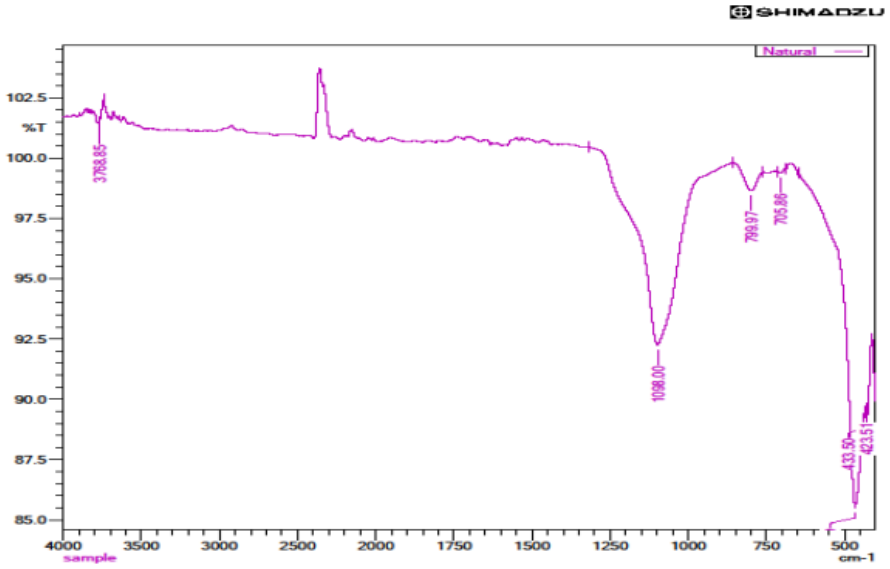

Figure 3. FT-IR spectrum for natural diatomite

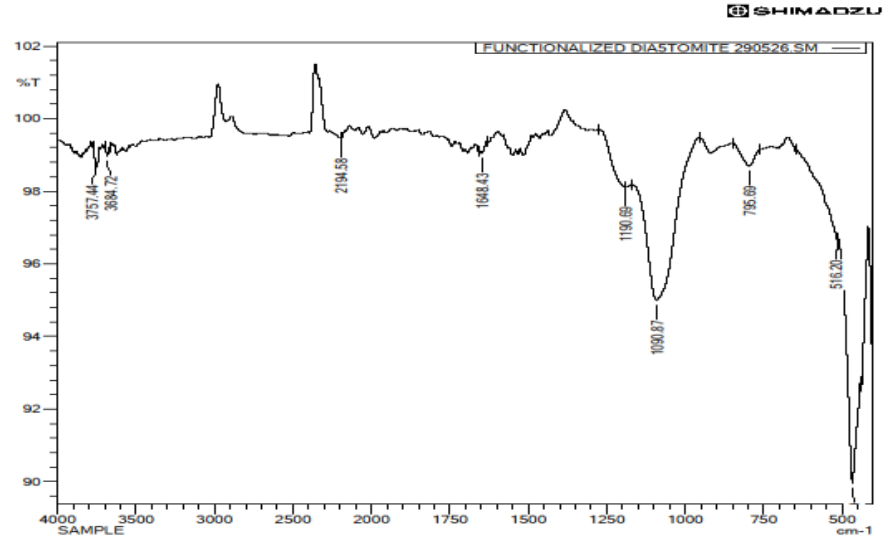

Figure 4. FT-IR spectrum for oxalic acid functionalized diatomite

3.2. X-ray Analysis of Natural and Functionalized Diatomite

The XRD analysis of both natural and functionalized diatomite was performed using the XRD D6 Phaser model. The analysis was performed to determine if the sample was crystalline or amorphous in nature and mineralogical composition. The results are represented in Figures 1 and 2, respectively.

The XRD of natural diatomite shows that raw diatomite contains mainly amorphous silica phase (Opal-A), which registers as a broad, diffused hump between 15 ° and 30 ° (2θ). The three crystalline peaks at (2θ) 23.952 °, 32.529 °, and 55.137 ° were observed. Traces of crystalline mineral impurities such as cristobalite, albite, and fluorite accompany diatomaceous materials with cristobalite being more abundant [8]. The dominant peak at 23.952 ° represents silica-rich phases, indicating the importance of the silica backbone, which plays a key role in its adsorption properties and porosity. It is found that both crystalline and amorphous silica co-exist, which allows the material to absorb pollutants like Pb (II) ions. Furthermore, the broad background hump seen in the diffractogram is consistent with the presence of amorphous silica that is important for adsorption applications.

Figure 2 shows that functionalization reduced the crystallinity of the diatomaceous material. The crystalline peaks reduced from three to one. The peak at (2θ = 24.755 °) is mainly attributed to cristobalite which is the main impurities in diatomaceous materials [8]. This indicates that the amorphous silica framework was maintained after functionalization. This diffractogram showed a high content of amorphous silica as an essential component to improve the high surface area and active adsorption sites [9]. The acid treatment enhanced the surface chemistry, making surface more amorphous and porous. This helps in improving the specific surface area that goes along in improving the

adsorption capacity of the composite by increasing adsorption sites. Overall, no structural changes were observed from the diffraction patterns in Figures 1 and 2.

3.3. FT-IR Analysis of Natural and Functionalized Diatomite

Fourier Transform Infrared (FT-IR) analysis was performed using a Shimadzu-119 instrument, calibrated after warming for 30 minutes with inactive potassium bromide. About 1mg of each powdered sample was mixed with potassium bromide in a 1:50 ratio, ground for homogeneity, and compressed into a translucent pellet. This pellet was then placed in the FT-IR machine for analysis, and the FT-IR spectrum was generated to interpret various peaks of interest. The spectrum for transmittance against wavelength for natural and functionalized diatomite is illustrated in Figures 3 and 4.

Based on Fourier transform infrared (FT-IR) analysis, the natural diatomite shows strong absorption peaks, which are associated with it being silica-rich. The wide bands in the range of 3400-3600 cm^{-1} are related to the hydroxyl group stretching modes, which are indicative of the hydrophilicity of surface silanol groups and adsorbed water. In addition, a peak at 3768.85 cm^{-1} is related to an isolated silanol group, indicating the presence of a high extent of hydroxyl functionalization for potential surface modification [9]. The strong band at 1098.00 cm^{-1}, which corresponds to the Si–O–Si vibration, indicates the prevalence of amorphous silica in the structure. Siloxane bridges are seen at a further peak at 799.97 cm^{-1} and at a small peak at 705.86 cm^{-1}, signifying minor crystalline silica is present. The intensity of the bands indicates that the silica lattice is well distorted at 433.50 and 423.51 cm^{-1}, corresponding to the low-frequency bands, which reveals the structural integrity of the material.

From Figure 4, there are notable changes on the FT-IR spectrum of the functionalized diatomite. The Si–OH bond is also closely coupled with a prominent peak at 3768.85 cm^{-1}, which undergoes a red shift to 3757.44 cm^{-1} after functionalization, suggesting a chemical bonding interaction. The presence of new peaks at 3684.72 cm^{-1}, 2194.58 cm^{-1}, and 1648.43 cm^{-1} is indicative of the properties of carboxylate groups ($–COO^{–}$) introduced from oxalic acid. The carboxylate group present is involved in ion complexation, especially with Pb^{2+} [4]. The peak at 1090.87 cm^{-1} corresponds to Si–O–Si stretching that exhibits shifts and additional shoulders, indicating interaction among the main structure of diatomite and the grafted oxalate that does not affect the main structure of diatomite. The disappearance of the peak at 433.50 cm^{-1} and 423.51 cm^{-1} related to Si–O and 705.86 cm^{-1} corresponding to Si–OH-forming bonds also helps to verify the successful modification of diatomite using oxalic acid.

3.4. Raman Spectroscopic Analysis

Raman spectroscopic analysis was performed using the ATR 3000-785 instrument at a wavelength of 785 nm to determine the structural modifications occurring upon the functionalization of Kariandusi diatomite with oxalic acid and to authenticate the anchorage of the oxalate functional groups. The results obtained are as shown in Figure 5 and Figure 6, respectively.

Figure 5 reveals that the primary composition of natural diatomite as amorphous silica, evidenced by a strong peak at 252 cm^{-1} linked to Si–O–Si lattice deformation. Additional bands at 2330 cm^{-1} for molecular CO_2 and 2697-2982 cm^{-1} for aliphatic C–H stretching indicating surface contaminants from organic matter present in natural diatomite.

Following oxalic acid functionalization, significant spectral changes were noted. The retention of the 250 cm^{-1} peak confirms the preservation of the silica framework, while the disappearance of the 2330 cm^{-1} band suggests reduced CO_2 adsorption. New bands at 2029 cm^{-1} and 2173 cm^{-1} signify the formation of oxalate-related surface species, enhancing the diatomite's capacity for heavy metal adsorption due to increased hydroxyl groups identified at 3276 cm^{-1}. Overall, the modifications led to improved adsorption performance while maintaining structural integrity.

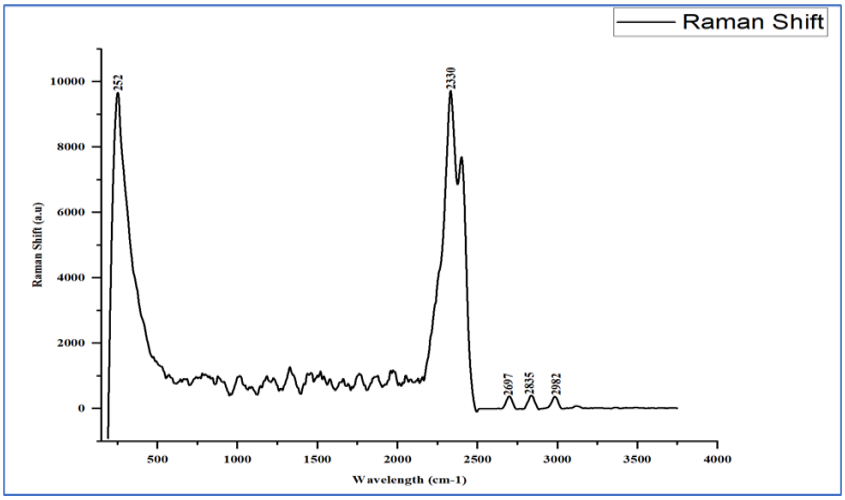

Figure 5. Raman spectrum for natural diatomite

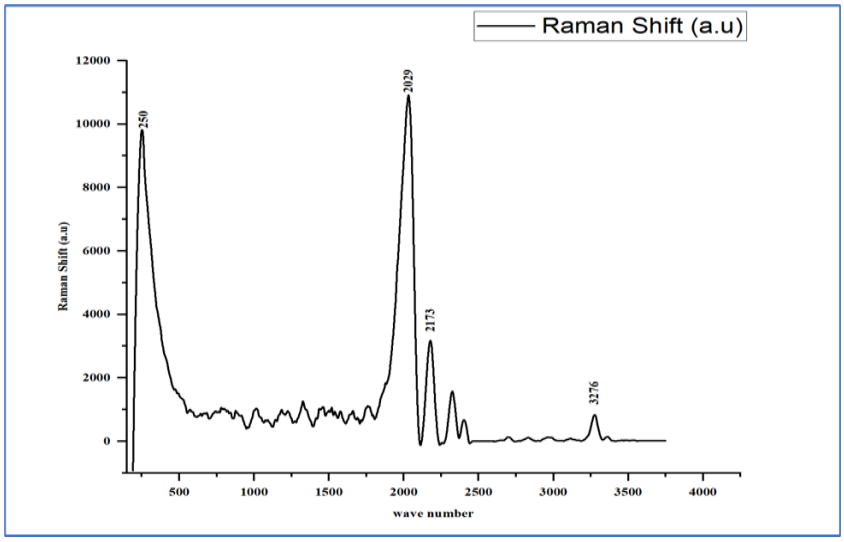

Figure 6. Raman spectrum for oxalic acid functionalized diatomite

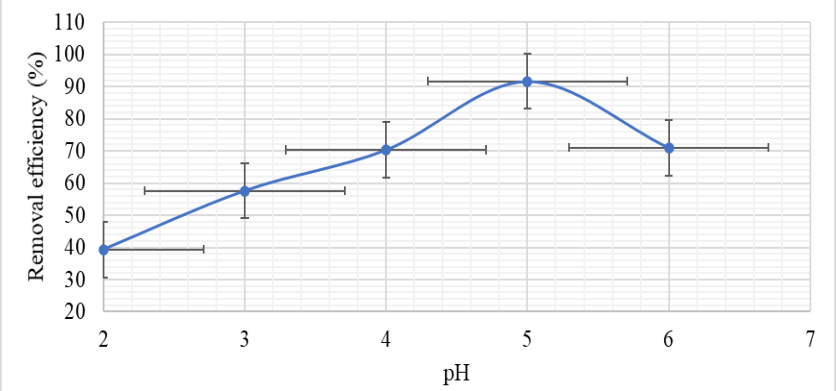

Figure 7. Effect of pH on adsorption of Pb (II) ions on functionalized diatomite

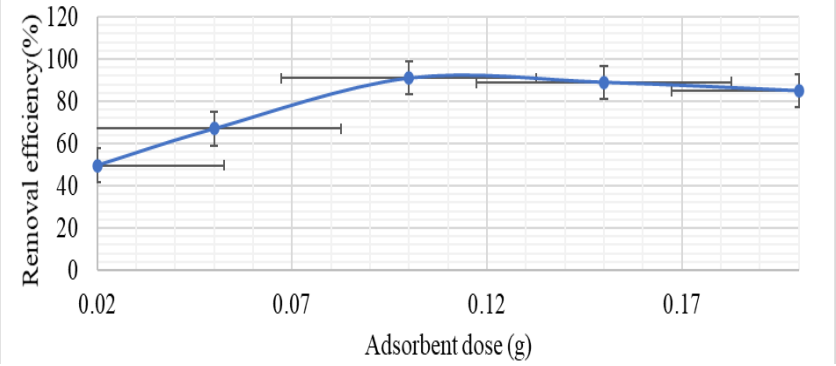

Figure 8. Effect of adsorbent dose on Pb $(II)^{+}$ ions removal efficiency using functionalized diatomite

3.5. Effect of pH on Adsorption of Pb (II) Ions Using Functionalized Diatomite

The batch experiments varied the pH from 2 to 6, with results depicted in Figure 7, showing the adsorption of Pb (II) ions using functionalized diatomite adsorbent.

Figure 7 shows that the removal efficiency increases with the increase in pH of wastewater until an equilibrium is attained at pH 5.0. When the pH is low, there are competing H^{+} ions for the adsorption sites, which means that fewer metal ions get removed. The increased pH value results in reduced competition and increased adsorption. However, beyond the pH level of 5.0, the removal efficiency decreases because hydroxide complexes are created, reducing the electrostatic interactions between the adsorbent surface and the molecules to be removed [10].

3.6. Effect of Adsorbent Dose on Adsorption of Pb^{2+} Ions

The experimental study involved varying the adsorbent dose from 0.02 g to 0.2 g to investigate the effect of adsorbent dose on the percentage removal efficiency of Pb (II). Other parameters were kept constant. At a shaking speed of 120 rpm, the results obtained are as illustrated in Figure 8.

The removal efficiency of the lead ions increased with an increase in adsorbent dose (49.67% at 0.02 g to 91% at 0.10 g), because an increase in the adsorbent dose increases the number of active sites. However, beyond this optimal dose, where the rate of adsorption becomes the same as the rate of desorption, the removal efficiency plateaued due to particle aggregation and reduction in the surface area, affecting the binding capability of the metal ions [11]. Low doses are ineffective due to the limited numbers of active sites and functional groups.

3.7. The Effect of Contact Time on the Removal Efficiency of Pb^{2+} on Adsorption Process

The study involved varying contact times from 10 to 120 minutes and a shaking speed of 120 rpm while other parameters were kept constant. The results obtained are as shown in Figure 9.

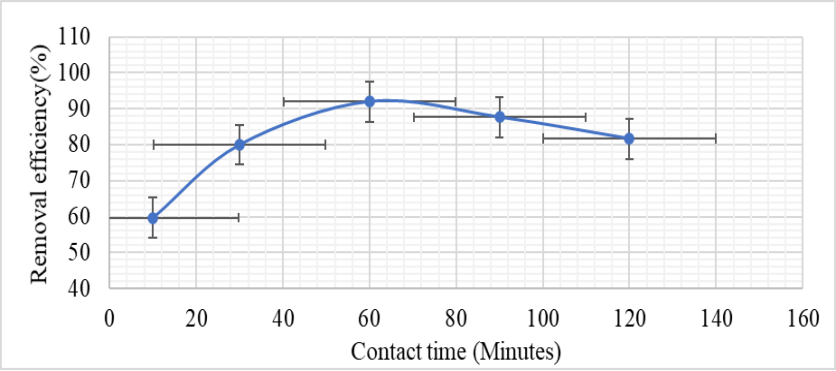

Figure 9. Effect of contact time on the removal efficiency of Pb2+ ions

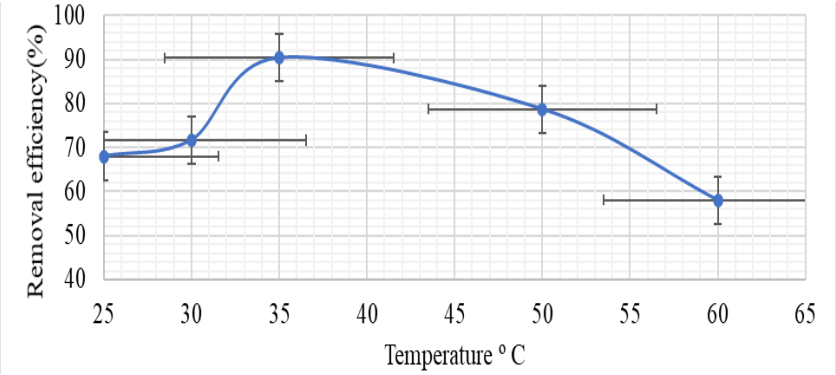

Figure 10. Effect of temperature on the removal efficiency of Pb (II) ions using functionalized diatomite

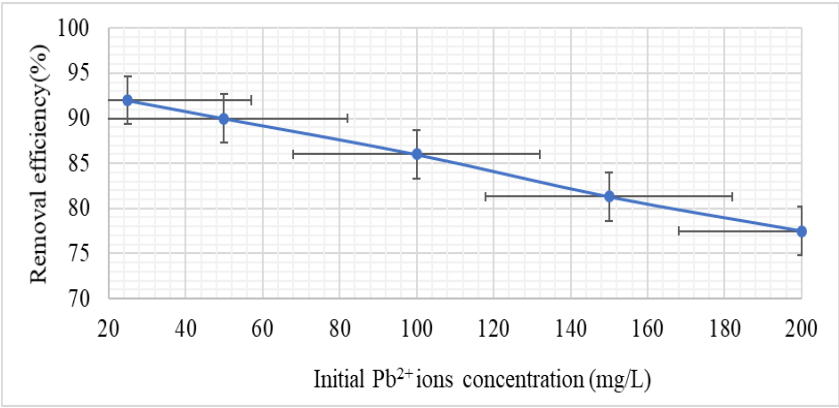

Figure 11. Effect of initial concentration on the removal efficiency of Pb (II) ions using functionalized diatomite

Table 2. Isotherm model constants and correlation coefficients for adsorption of Pb (II) ions onto functionalized diatomite adsorbent

	Langmuir Isotherm			Freundlich Isotherm		
Metal ion	K_L	Q_{max}	R^2	1/n	K_F	R^2
Pb (II) ion	0.0534	106.3830	0.9869	0.6107	8.0057	0.9942

1/n = heterogeneity index, K_F =Freundlich constant, R^2= correlation coefficient, Q_{max}= adsorption capacity, K_L = Langmuir constant.

The results show that the removal efficiency of Pb (II) ions increased with an increase in contact time, attaining equilibrium at 60 minutes with an optimal removal efficiency of 92%. An increase in the removal efficiency could be attributed to strong electrostatic attractions and surface complexation that enhanced the mass transfer of Pb (II) ions to the adsorbent. The functionalization of the adsorbent with oxalic acid introduces reactive groups that facilitate this interaction. Initial rapid adsorption is followed by a slower equilibration as binding sites fill, demonstrating that the adsorption process is primarily surface-based. Beyond 60 minutes, the removal efficiency declines slightly, linking to desorption due to weak interactions and possible structural changes in the adsorbent [12]. The findings highlight the importance of operational efficiency in wastewater treatment by achieving equilibrium in a shorter time.

3.8. The Effect of Temperature on Adsorption

The study specifically examined the effect of temperature (25-60 ℃) on the percentage removal of Pb (II) ions at a starting concentration of 100 mg/L, using an adsorbent dose of 0.1 g/50 mL and a shaking speed of 120 rpm, with results illustrated in Figure 10.

From Figure 10, an increase in temperature increases the adsorption efficiency of Pb (II) ions. Removal efficiency increased when temperature was varied from 25 ℃, attaining an optimal efficiency at a temperature of 35 ℃. An increase in temperature increases kinetic energy, which in turn increases ion mobility that facilitates stronger interactions with adsorbent functional groups. This optimal range allows for effective metal removal at near ambient temperatures, reducing operational costs. Beyond 35 ℃, the efficiency declines due to the exothermic nature of the process, promoting desorption rather than adsorption [13].

3.9. The Effect of Initial Concentration on Adsorption

The effect of initial metal ion concentration on the percentage removal was investigated by varying the concentration of Pb (II) ions from 25 mg/L to 200 mg/L, using an adsorbent dose of 0.1 g/50 mL and a shaking speed of 120 rpm, with results illustrated in Figure 11.

From Figure 11, the removal efficiency of Pb (II) ions decreases with an increase in initial ion concentration (92% at 25 mg/L to 77.5% at 200 mg/L) under the same conditions. This trend is attributed to the exhaustion of available adsorption sites as concentration increases, leading to competition among ions. Overall, oxalic acid functionalized diatomite proves to be an efficient adsorbent, particularly at low concentrations where more active sites are available.

3.10. Adsorption Isotherms

The adsorption data for Pb (II) ions were fitted onto both Langmuir and Freundlich isotherms. The isotherm constants and correlation coefficients obtained are tabulated in Table 2.

Table 2 shows that the adsorption data for Pb (II) ions onto oxalic acid-functionalized diatomite fit well in Freundlich models with $R^2 = 0.9942$, which is higher than $R^2 = 0.9869$ for the Langmuir model. The R^2values indicate strong linear relationships. This is indicative that adsorption occurred on a heterogeneous surface structure of the adsorbent. The heterogeneity index (1/n) values for Pb (II) ions (0.6107) confirm high favorable uptake.

4. Conclusions

The study successfully functionalized diatomite with oxalic acid to enhance its ability to adsorb Pb (II) ions from wastewater. Characterization techniques, including XRF, XRD, FT-IR, and Raman spectroscopy, confirmed that the functionalization altered the chemical composition and introduced oxygen-containing functional groups without changing the amorphous silica structure. The batch sorption experiments showed that the adsorption process was dependent on adsorption parameters. The findings suggest that oxalic acid-functionalized diatomite is a potentially effective, eco-friendly, and cost-efficient adsorbent for Pb(II) ion remediation from wastewater.

Conflict of Interests

The authors declare that they have no known competing financial interests or personal relationships that could appear to have influenced the work described in this paper.

ACKNOWLEDGEMENTS

The authors express gratitude to the Department of Science Technology and Engineering, Kibabii University's for the assistance offered during the whole of research period.

REFERENCES

[1] Ngatia, M., Kithiia, S. M., & Voda, M. (2023). Effects of Anthropogenic Activities on Water Quality within Ngong River Sub-Catchment, Nairobi, Kenya. Water, 15(4), 660.

[2] Mansour, H., Nassar, H. F., Zaghloul, A., Kabary, H., & Ahmed, S. A. (2025). Preparation and evaluation of altered zeolite and diatomite as affordable adsorbents in contaminated water treatment. Applied Water Science, 15(7), 160.

[3] Galzerano, B., Aprea, P., Verdolotti, L., De Luna, M. S., Ascione, C., Caputo, D., & Liguori, B. (2021). Effect of carbonaceous fillers on adsorption behaviour of multifunctional diatomite-based foams for wastewater treatment. Chemosphere, 281, 130999.

[4] Rinila, R. T. O., Yong, S. K., Al-Amrani, W. A., Wibowo, A., Ghazali, N. F., Yılmaz, M., Suah, F. B. M., & Megat Hanafiah, M. A. K. (2025). Efficient recovery of Ce (III) ions from acidic solutions using oxalic acid crosslinked chitosan. Results in Surfaces and Interface, 18100445.

[5] Maingi, F. M., Mbuvi, H. M. Ng'ang'a, M. M. Mwangi, H. (2018). Adsorption of Cadmium Ions on Geopolymers Derived from Ordinary Clay and Rice Husk Ash. International Journal of Materials and Chemistry, 2018, 8(1): 1-9.

[6] Maingi, F. M., Mbuvi, H. M. and Ng'ang'a, M. M. (2016). Remediation of Water Contaminated with Cr6+ and Cd2+ Using Aluminophosphates Derived from Ashes of Tea Leaves and Pumpkin Seeds. Journal of Chemistry and Material Research, Vol 8(7) 94 – 102.

[7] Maingi, F. M., Mbuvi, H. M., Mwangi, H. and Ng'ang'a, M. M. Clay-Rice Husk Ash based Geopolymers for Remediation of Pb (II) and Cd (II) from Wastewater Egerton Journal of Science & Technology, 2019 Oct Volume 17: 15-28.

[8] Dinh, Q. T. (2025). Characteristics, origin, and application potential of Diatomite at Lam Ha ward, Lam Dong province. Inżynieria Mineralna, 2(1), 326-338.

[9] Eurov, D. A., Kurdyukov, D. A., Nechitailov, A. A., Krasnodar, A. O., Mazur, A. S., & Stovpiaga, E. Y. (2025). Structure-stabilizing silanols in amorphous silica with ultra-high specific surface area. Colloids and Surfaces A: Physicochemical and Engineering Aspects, 725, 137523.

[10] Ismail, W. W., Syah, M. I. A. I., Muhet, N. H. A., Bakar, N. A., Yusop, H. M., & Samah, N. A. (2022). Adsorption behavior of heavy metal ions by hybrid inulin-TEOS for water treatment. Civil Engineering Journal, 8(9), 1787-1798.

[11] Bahera, A. K., Shadangi, K. P., & Sarangi, P. K. (2024). Efficient removal of Rhodamine B dye using biochar as an adsorbent: Study the performance, kinetics, thermodynamics, adsorption isotherms.

[12] Thamarai, P., Deivayanai, V. C., Swaminaathan, P., Karishma, S., Vickram, A. S., & Yaashikaa, P. R. (2024). Experimental investigation of Cd (II) ion adsorption on surface-modified mixed seaweed Biosorbent: A study on analytical interpretation and thermodynamics. Environmental research, 260, 119670.

[13] Dehghani, M. H., Afsari Sardari, S., Afsharnia, M., Qasemi, M., & Shams, M. (2023). Removal of toxic lead from aqueous solution using a low-cost adsorbent. Scientific reports, 13(1), 3278.